

Thin-film barrier on foil for organic LED lamps

Ferdie van Assche*, Harmen Rooms, Edward Young, Jasper Michels, Ton van Mol
Holst Centre/TNO, High Tech Campus 31, 5656 AE, Eindhoven, the Netherlands

Gerard Rietjens, Peter van de Weijer, Piet Bouten
Philips Research Laboratories, High Tech Campus 4, 5656 AE Eindhoven, the Netherlands

Abstract

Within the Holst centre a transparent barrier on foil has been under development which is based on low-temperature plasma deposited silicon nitride films as intrinsic moisture barrier, stacked with planarization layers to spatially separate defects in these films. OLED lifetime testing and water vapor transmission rate measurements using a Ca-mirror test have been performed, and the barriers have been submitted to strain and cyclic bending tests to assess their feasibility within a roll to roll production environment.

1. Introduction

One of the most important factors determining the lifetime of organic light emitting diodes (OLEDs) is degradation due to moisture from the environment. The low work function materials used as cathode oxidize rapidly when getting into contact with water. In addition, the polymer and organic materials used in OLEDs may degrade as well. Therefore, to achieve feasible lifetimes the devices have to be sealed from the ambient atmosphere. For non-flexible applications of OLEDs the use of glass or metal lids in combination with encapsulated getter materials, has been proven a feasible method [1]. However, barrier on foil and thin film encapsulation have been under widespread investigation [2] [3] as they enable production of thinner and lighter devices, the use of flexible substrates, and more cost-effective roll-to-roll production of OLEDs.

At least three types of OLED degradation due to moisture can be distinguished: i) an overall intrinsic water vapour transmission rate (WVTR) of a barrier may result in a reduced light output; ii) local black spot formation may occur due to water leakage through generally ever-present pinholes in an otherwise hermetic Al cathode or ITO anode layer; iii) lateral diffusion paths for water through the polymer layers may be a cause of a third type of degradation.

Lighting applications of OLEDs can be considered more forgiving than display applications with respect to some moisture barrier properties. For instance, an overall reduction in luminescence as well as the presence of small black spots may be acceptable within the lifespan of a lighting panel, as neither are easily detectable by the human eye and lighting devices are not produced to continuously look at directly. However, to prevent visible black spots within a lifetime of 10 years the maximum acceptable WVTR has been empirically estimated at a maximum of 10^{-6} g/m²day, as deduced from the black spot growth rate of an OLED that has been covered with a barrier with known WVTR [4]. Further demands to the barrier include optical transparency and feasibility for large scale industrial production, i.e. high deposition rates and large area processing. While flexibility or one-time-bending ability of the device may be an interesting but not necessary asset for the end-product, flexibility of the barrier is required for enabling roll-to-roll processing for a more cost-effective production. To an even larger extent than for display applications, cost-effectiveness is of key

importance to enable entrance of OLEDs into the lighting market.

At the Holst Centre [5], a moisture barrier on foil has been under development which is based on amorphous hydrogenated silicon nitride (a-SiN_x:H) films as the actual barriers, and an organic planarizing interlayer for decoupling of defects. To assess the feasibility of this barrier in a roll-to-roll production environment, both individual a-SiN_x:H films and whole barriers have been submitted to mechanical tests. The crack channeling strain, i.e. the amount of strain that results in extension of a crack or defect in a film across the film, of used materials in a barrier stack is one of the parameters that determine the minimum radius to which a barrier may be bent before failure occurs. Therefore, the crack channeling strain of single a-SiN_x:H films, the most brittle material in the stack, has been determined. The performance of a complete barrier has been tested before and after repetitive bending.

2. Lifetime and mechanical testing of barriers

2.1. The Ca-mirror test

For testing moisture barriers, a Ca-mirror test has been used, as described in [6]. In this testing method, a Ca film of typically 40 nm thickness is encapsulated using the tested (transparent) barrier. As Ca is opaque and CaO is transparent, the amount of water traversing the barrier can be determined by monitoring the transparency of an oxidizing Ca film. Using this method, WVTR values down to 10^{-6} g/m²day or lower can be measured, depending on the measurement time available.

2.2. Critical strain testing of a-SiN_x:H

A method of determining the crack channeling strain as developed by Bouten, Leterrier e.a. [7] has been applied to measure the tensile strength of plasma deposited 300 nm thick a-SiN_x:H films, deposited on a 125 μm thick PEN foil at a low substrate temperature (100-150°C) using a 13.56 MHz RF driven parallel plate reactor.

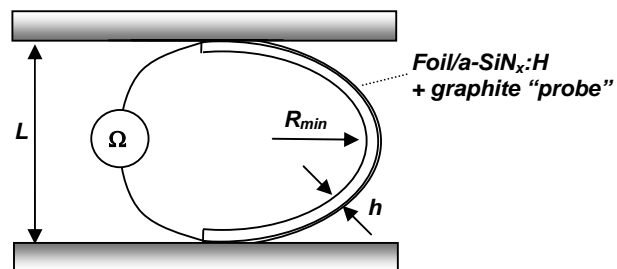


Figure 1: Crack channeling strain measurement setup. A thin graphite layer is used to electrically detect fracture of the non-conductive a-SiN_x:H film.

A 10x1.5 cm² piece of foil with a-SiN_x:H has been bent between two parallel plates mounted on an Instron 5566 tensile testing machine. On top of the a-SiN_x:H film an

* Ferdie.vanAssche@tno.nl, phone +31 40 2774344; fax +31 40 2746400 ; www.holstcentre.com

additional very thin (<10 nm) graphite film is deposited to serve as a conductive probe film. As the graphite film is both very thin and brittle, cracks in the a-SiN_x:H film will induce fracture of the graphite film. Hence by monitoring the resistance of the graphite film, fracture of the a-SiN_x:H film can be detected. Crack channeling strain values as obtained by this method have shown excellent agreement with those obtained by a more elaborative optical detection of fracture [8].

The maximum tensile strain ϵ_{max} due to bending occurs at the outer side, at the smallest radius in the middle of the bend, and is for a symmetrical foil given by

$$\epsilon_{max} = \frac{c_b h}{L} \quad (1)$$

with h the thickness of the foil, L the plate distance, and $c_b=1.198$ a geometrical constant accounting for the fact that the bending shape is not circular. The setup is computer-controlled, such that the resistivity of the graphite film can be related to the plate distance.

2.3. Cyclic bending test

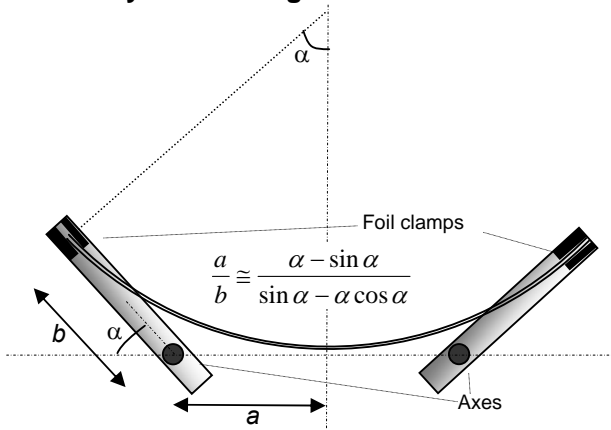


Figure 2: Two-point cyclic bending test setup. The foil can be bent in both directions without contacting the surface.

For bending testing of complete barrier stacks on foil, a test setup has been used consisting of a custom made bending device in which a foil can be bent in both directions such that the barrier on the foil endures both compressive and tensile strain, without touching the barrier surface. The dimensions a and b as shown in Figure 3 are chosen such that the foil shape is approximately circular. In the tests that have been applied, 5-100 successive bendings have been performed in both compressive and tensile mode, down to a radius of 14 mm.



Figure 3: Stack configuration for the bending test.

Before and after bending the foils, the WVTR and defect density of the barriers have been measured by using a Ca-mirror test. The configuration of the tested and bended substrates is depicted in Figure 3. A patterned 40 nm thick Ca film is surrounded by barriers both below and above the Ca on top of a 125 μm thick PEN foil of $\sim 5 \times 10 \text{ cm}^2$ size.

3. Experimental results

3.1. Crack channeling strain of a-SiN_x:H

In Figure 4 the increase in resistance of the graphite probe film on top of a 300 nm a-SiN_x:H film on PEN is shown as a function of the applied strain for a series of identical films.

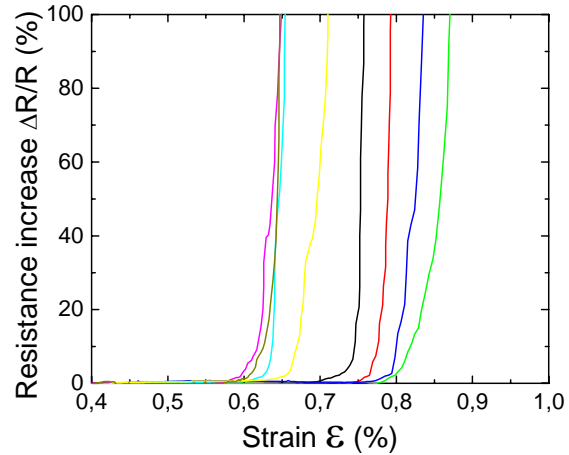


Figure 4: Resistance increase of probe layer on top of a 300 nm thick a-SiN_x:H film on PEN foil as a function of the tensile strain. Crack extension occurs at strains from 0.6-0.8%

As visible from the graph, the resistance is constant initially, indicating that the films remain intact for bending strains up to 0.6-0.8%, corresponding to a bending radius of ~ 11 mm for the employed PEN substrate thickness of 125 μm . Further bending results in fracture of the a-SiN_x:H films and rapid increase of the resistivity of the probe film. This measurement is in reasonable agreement with previously reported critical strain values of 0.4-0.5% for plasma deposited a-SiN_x:H films on poly-imide coatings [9].

3.2. WVTR of barrier stacks on foil

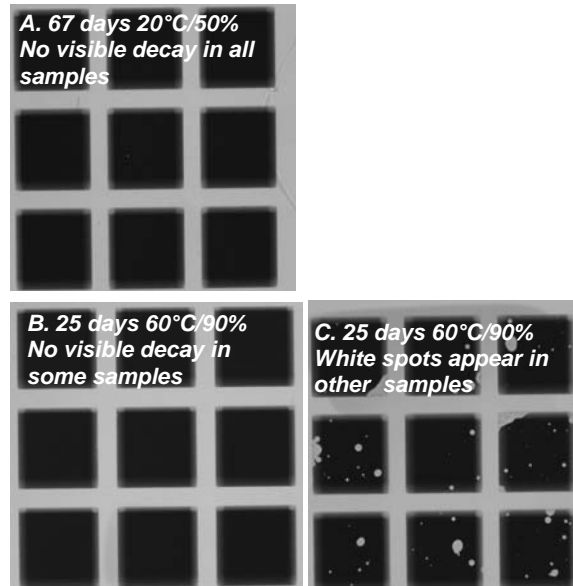


Figure 5. Ca-mirror test of the barrier. A: 67 days testing, WVTR <math><10^{-5}</math> g/m²/day at 20°C/50% (ongoing). B: 25 days testing, WVTR =5·10⁻⁵ g/m²/day at 60°C/90%. C: After three weeks at 60°C/90% white spots appear in most samples.

Barriers on foil have been submitted to the Ca-mirror test, using the same configuration as in Figure 3.

For barriers using a-SiN_x:H recipes that have been developed for low temperature deposition, 5·10⁻⁵ g/m²day has been measured during storage in a 60°C/90%rH environment for accelerated testing. After three weeks, white spots appear in some of the samples at these accelerated test conditions, as shown in Figure 5B and 5C. Some samples are still spotless though. The water vapor partial pressure in a 60°C/90%rH environment is approximately 15 times higher than at ambient conditions (20°C/50%rH). However, this does not necessarily mean that at ambient conditions a 15 times longer lifetime may be expected, as the lifetime of three weeks might be partly caused by a diffusion delay in the barrier.

The 20°C/50%rH test is ongoing, and does after two months not yield a measurable WVTR which is well below 10⁻⁵ g/m²day. No white spot formation has taken place after 2 months, as shown in Figure 5.

3.3. Cyclic bending of a barrier stack

For the initial bending tests, a non-optimized barrier stack has been used, yielding average WVTR values of 8·10⁻⁵ g/m²day at room conditions. In Figure 6 the ratio of the measured WVTR of several samples before and after cyclic bending is shown as a function of the applied bending radius, as well as for varying amounts of bending cycles. For a parallel batch of unbended barriers, an unexplained WVTR ratio below 1 has been measured, which suggests an in time reducing water flux, but is more likely a result of a non-linearity in the transparency of the Ca at the initial stage of oxidation.

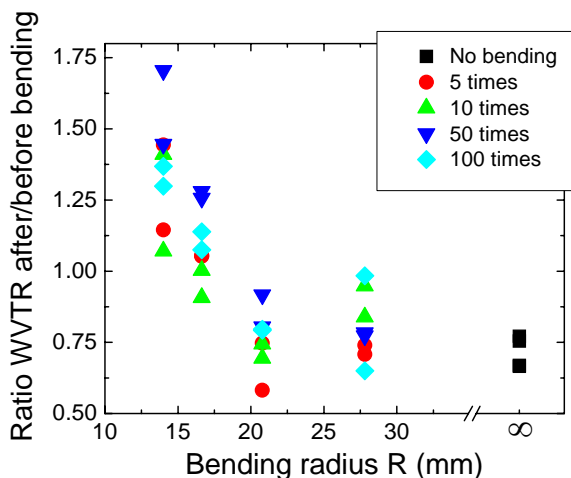


Figure 6: Increase in WVTR (ratio after/before bending) as a function of the bending radius. Only at radii below 20 mm a significant increase in the WVTR is observed

The trend in Figure 6 indicates that the WVTR is not affected for bending radii down to ~20 mm. There is no clear dependence on the number of bending cycles during the test, indicating that if damage results from the bending, this already happens during the initial bending cycles, while no further damage results from further bending. After 80 days continued climate testing at 20°C/50% after the bending, no white spots have appeared, even for the barriers that have been bent below a 20 mm radius. Bending tests on an optimized barrier

stack are currently ongoing.

4. Conclusion

The WVTR of a SiN-org-SiN barrier stack on foil has been shown to be well below <10⁻⁵ g/m²day at ambient conditions without visible defects in a Ca-mirror test for 67 days, and is ongoing. At 60°C/90%rH a WVTR of 5·10⁻⁵ g/m²day has been measured for the top and bottom stack together.

Using a two point bending test in combination with a conductive probe layer, a crack channeling strain for a-SiN_x:H of 0.6-0.8% has been measured for 300 nm thick films. This measurement is in line with previously reported values for a-SiN_x:H on poly-imide substrates [9].

The tested barriers have been shown to withstand bending radii down to ~20 mm, which is a small enough radius to enable roll-to-roll processing.

5. Acknowledgements

The Holst Centre is an open innovation research centre founded by TNO and IMEC that is developing roll-to-roll production techniques for foil-based organic electronics and wireless autonomous transducer solutions, in cooperation with industry and universities. This particular research has been funded by the Dutch Ministry of Economic Affairs, Philips Research, OTB Display, Bekaert and Huntsman.

The experimental work has been performed in the Philips Miplaza research facilities. The deposition of barrier layers has been performed in the pre-pilot line of the Device Process Facilities, with thanks to Jan Jansen, Paul Aerts and Jan Manders. Pieter Klaassen and Marc Kuilder of the Philips Research reliability center are acknowledged for the Ca-mirror measurements.

6. References

- Burrows, P.E., et al., *Reliability and degradation of organic light emitting devices*. Appl. Phys. Lett., 1994. **65**(23): p. 2922-2924.
- Assche, F.J.H.v., et al., *A Thin Film Encapsulation Stack for PLED and OLED Displays*. Society for Information Display (SID) International Symposium, 2004. **35**: p. 695-697.
- Chwang, A.B., et al., *Thin film encapsulated flexible organic electroluminescent displays*. Appl. Phys. Lett., 2003. **83**(3): p. 413-415.
- Peter van de Weijer et al., *Thin-film encapsulation of organic LEDs*. Organic Semiconductor Conference, 2008. Frankfurt.
- See also: www.holstcentre.com
- Nisato, G., et al., *Evaluating High Performance Diffusion Barriers: the Calcium Test*. 21st Annual Asia Display, 8th International Display Workshop, 2001: p. 1435-1438.
- Letierrier, Y., et al., *Models and Experiments of Mechanical Integrity for Flexible Displays*. Society for Information Display (SID) International Symposium, 2008: p. 310-313.
- Bouten, C.P., et al., *Mechanics of ITO on Plastic Substrates for Flexible Displays*, in Flexible flat panel displays, John Wiley & Sons, 2005: p. 528.
- Andersons, J., et al., *Evaluation of toughness by finite fracture mechanics from crack onset strain of brittle coatings on polymers*. Theoretical and Applied Fracture Mechanics, 2008. **49**: p. 151-157.